Comparative Study on the Combustion and Emissions of Waste Tire Crumb and Pulverized Coal

ARTICLE *in* ENVIRONMENTAL SCIENCE AND TECHNOLOGY · AUGUST 1996

Impact Factor: 5.33 · DOI: 10.1021/es950910u

5 AUTHORS, INCLUDING:

Yiannis Levendis
Northeastern University
113 PUBLICATIONS **1,988** CITATIONS

SEE PROFILE

Environ. Sci. Technol. **1996**, *30,* 2742−2754

Comparative Study on the Combustion and Emissions of Waste Tire Crumb and Pulverized Coal

YIANNIS A. LEVENDIS,*,† AJAY ATAL,† JOEL CARLSON,‡ YURY DUNAYEVSKIY,‡ AND PAUL VOUROS‡

Department of Mechanical Engineering and Department of Chemistry, Northeastern University, Boston, Massachusettes 02115

Comparative results are presented on the combustion and toxic emissions (SO_2, NO_x, CO, and PAHs) from a pulverized bituminous coal and ground waste automobile tires. The combustion behavior of single particles in the range of 60−212 μm was monitored pyrometricaly and cinematographically, at a gas temperature of 1150 °C and a heating rate of $\approx 10^5$ °C/s. Tire particles burned faster (by a factor of 2−3) than similar size coal. Coal particles experienced distinct devolatilization and char combustion stages. Upon intense volatile combustion, the chars of tire particles burned accompanied by secondary devolatilization that aided the burnout of their carbon black residue. No soot appeared to escape the volatile flame envelope. The SO_2 emissions from the combustion of steady-flow clouds (aerosols) of tire and coal particles were comparable (within a factor of 2), the NO_x emissions of tires were lower than those of coal by a factor of 3−4, reflecting their lower fuel nitrogen content. Insignificant amounts of CO were detected in the effluent of both fuels at fuel-lean or stoichiometric conditions. CO sharply increased in fuel-rich combustion, while NO_x emissions decreased. No polynuclear aromatic hydrocarbon (PAH) emissions were detected in the effluent of fuel-lean and stoichiometric combustion of clouds of coal particles at a furnace gas residence time of 0.75 s. Even at mildly fuel-rich conditions, $1.0 < \phi < 1.8$, only small amounts of PAHs were detected in the effluent of burning coal particles. At higher equivalence ratios, ϕ, PAH emissions increased sharply. Combustion of clouds of tire particles produced no detectable PAHs at $\phi < 0.6$, but as stoichiometry was approached or exceeded, the PAH emissions increased substantially. Thus, the onset of detectable PAH emissions occurred at lower ϕ for tires than for coal. Beyond that point, the PAH emissions of both fuels increased exponentially in fuel-rich combustion, asymptotically reaching the pyrolytic gas-phase PAH emissions in N_2. Individual gas-phase PAH emissions of tires were 1.5−2 times higher than those of coal at comparable fuel-rich ϕ and were 1.5−10 times higher under pyrolytic conditions, where maximum amounts were recorded. Similar trends were observed in the condensed-phase PAH emissions of both fuels; however, the highest yield was obtained under oxygen-starved oxidative environments. Differences in the PAH emission tendencies of the two fuels were amplified when combustion took place in fixed beds. Coal burned relatively clean, while tire crumb emitted copious amounts of smoke and PAHs, with individual compounds dramatically exceeding (by 10−100 times) those from burning pulverized coal.

Introduction

Coal is the predominant fuel for power generation in the world. The United States alone produces 1.0 ± and consumes approximately 0.8 billion t of coal yearly for power generation. Thus, a thorough study of the emissions of coal is warranted. Waste tires, on the other hand, are generated by the billions every year, with the United States alone discarding an estimated quarter of a billion tires, but they are not currently used for energy generation to any significant extent. Instead, they are either landfilled or stored in tire dumps, creating health problems and fire hazards. Because of their high heating value (29−37 MJ/kg, which is higher than most coals), however, waste tires are being considered as an attractive potential fuel. With an average weight for tires of 10 kg, a total of 2.5 million t of tire-derived fuel can be produced in the United States per year amounting to 0.3% of the coal consumption. In addition to this amount, more fuel can be deduced from existing tire stockpiles, and the yearly electric energy production potential from tires could reach 1% of that from coal.

While pulverized coal is widely used in most utility-fired boilers, pulverized rubber from waste tires is still a costly proposition, mainly because of the cryogenic processes that are currently used to produce it and the small scale of existing operations. According to certain sources (*1*, *2*), the current price of pulverized tires is currently 3−5 times higher than that of coal (180−300 vs 60 U.S. dollar/t). This price differential may be bridged, however, if cost-effective large-scale tire grinding processes are invented and/or if higher disposal fees are implemented. Thus, tire crumb may be considered as a supplemental fuel in already existing pulverized coal boilers. This will avoid the high cost of building dedicated tire-to-energy combustion facilities (*3*). With this reasoning in mind, the present work examined the combustion and emissions of both fuels in *pulverized* form. However, regardless of the economics of pulverizing tires, burning the two fuels in the size scale of

* Corresponding author telephone: (617)373-3806; fax: (617)373-2921; e-mail address: yal@artemis.coe.neu.edu.

† Department of Mechanical Engineering.

‡ Department of Chemistry.

 S0013-936X(95)00910-2 CCC: $12.00

small particles facilitated a fundamental-level comparison of their combustion characteristics (see also ref 4) and emissions in the limited dimensions of laboratory bench-scale equipment. Development of a process to produce tire crumb and an economic feasibility study are currently being conducted at Northeastern University.

Review of Literature

Combustion Behavior. The combustion characteristics of pulverized coal have been extensively studied elsewhere (see reviews in refs 5−8), but little has been reported on the combustion of ground tires (*9*−*12*). A comparison on the combustion characteristics of single particles (80−200 μm) of both fuels was recently conducted in this laboratory, under high heating rates (10^5 °C/s) (*4*). In that study, separate volatile and char combustion phases were detected for the coal particles examined. Tire particles experienced an intense primary volatile combustion phase, followed by a phase of secondary evolution and burning of volatiles, of lesser intensity, and simultaneous char combustion. During the initial volatile phase combustion, the peak flame temperatures were comparable for both materials and were in the range of 2200−2400 K at a gas temperature of 1450 K (1177 °C). The secondary volatile/char combustion phase observed for the tire particles was cooler, i.e., 2000−2100 K. The coal chars burned even cooler, with surface temperatures of 1850−2000 K. Combustion was found to be diffusionally controlled (Regime III (*5*)). Char burnout times were much shorter for tire particles than for coal particles of the same size, which can be attributed to the secondary devolatilization and the lower density of the former. Combustion results pertinent to the particle sizes used in the present study are given at a subsequent section. A study on the combustion of particles of both fuels burning in clouds (see Figure 3) is currently being undertaken.

Combustion Emissions. The most important emissions from the combustion of coal and tires are the inorganic gases SO_2 and NO_x, submicron metal aerosols (fumes), and toxic organic emissions, such as polynuclear aromatic hydrocarbons (PAHs), soot, and CO. Of recent concern are also the emissions of CO_2.

NO_x−SO_2 Emissions. Extensive literature exists on the SO_2 and NO_x emissions from the combustion of coal and on the methods for their control, see for instance refs 13−16. The emitted sulfur-bearing gases have been found to be nearly quantitatively proportional to the sulfur content of the coal. The amount of nitrogen oxides emitted is also mostly attributed to the fuel-bound nitrogen, with the thermally-fixated atmospheric nitrogen playing a minor role, see reviews by Bowman (*14*), Flagan and Seinfeld (*16*), and Sarofim and Bartok (*15*). Pershing and Wendt (*17*) tested five coals and found that fuel nitrogen always contributed more than 75% of the total NO that was generated. Yet, less than 30% of the fuel nitrogen was converted to NO. Limited work has addressed such emissions from the combustion of tires. For instance, SO_2−NO_x emissions from co-firing whole tires with pulverized coal in a modified 42 MW wet-bottom Ohio Edison boiler were monitored by Horvath (*18*). Tires were introduced to the boiler at varying feed rates and thus, the mass fraction of tires as a fuel varied from 0 to 1. It was reported that co-firing whole tires with coal reduced stack emissions of SO_2, NO_x, and particulates. Neither the chemical composition of coal and tires used nor the firing conditions were given in that report. Tire burn tests and associated SO_2−NO_x emissions were also mentioned by Pope (*19*) and in two articles appearing in *Power* (*20*, *21*). However, due to the complexity of the tests in utility furnaces, little fundamental understanding has been gained. In a recent study, the authors examined the SO_2 and NO_x emissions of tires in pulverized form in laboratory-scale experiments and found that, while the CO_2 and SO_2 emissions were comparable to those from coals burned in the laboratory, the NO_x emissions from tires were much lower (*22*).

Polynuclear Aromatic Hydrocarbon Emissions. Work on the toxic organic emissions, volatile organic compounds (VOC), and semivolatile organic compounds (SVOC), a subset of which are the polynuclear aromatic hydrocarbons (PAHs), of coal and especially tires is limited. While at present CO_2, CO, and total volatile hydrocarbons can be monitored on-line by a variety of analyzers, techniques are not available to continuously monitor and quantify individual organic products of incomplete combustion (PICs), primarily the PAHs. Investigations are further complicated due to the large number of organic compounds that are formed as a result of incomplete combustion of fuels such as coal, oil, tires, etc. and the labor-intensive process for their detection. The importance of identification and quantitation of many PAHs arises from the known carcinogenic nature of some of these compounds. For some fuels, such as coal or hydrocarbon fuel blends (like diesel oil), emitted PAHs may be directly traced to the fuel composition or may be formed from the combustion reaction (pyrosynthesis) (*23*−*30*). Also, the formation of PAHs is highly dependent on the conditions existing in the vicinity of burning fuel (*31*).

Several studies have reported on PAH emissions from coal-fired power plants (*31*, *32*), while others have reported on PAH emissions of coal burning under more controlled conditions in experimental furnaces (*23*, *33*). Masclet and co-workers (*31*) found that the coal type has a bearing on the type and amount of PAHs produced. No correlation between the rank of coal and PAH emissions could be obtained as differences between two different coals burning under similar conditions were unevenly distributed with regard to lighter vs heavier PAHs. Of the two coals tested therein, the higher volatile content coal produced light PAH compounds while the other coal, which contained more minerals, produced a larger amount of high molecular weight PAHs. Bonfanti et al. (*23*) on the other hand found that the coal type hardly affected the types and amount of PAHs formed. Changes in the combustion conditions—temperature and mixing—can alter the level and composition of the PAH compounds. Under normal operating conditions, mostly 2 ring compounds were detected, but when the optimal mixing condition worsened, a predominance of 4−7 ring compounds was seen. Garcia et al. (*32*) also concluded that the effect of coal type was much less important than that of furnace design and load power on the emissions of PAHs. Miller et al. (*33*) studied the combustion of a bituminous coal and the resulting hazardous organic pollutants in a small-scale combustor. The emissions were analyzed under three different conditions—baseline, fuel-lean, and a low-NO_x configuration (gas temperatures for these conditions were not provided). The emissions of targeted organic pollutants from the combustion of coal were found to be low under fuel-lean conditions and showed an increase when the low-NO_x configuration was used. To the contrary, Nsakala et al. (*34*) did not detect much difference in the amount of PAHs emitted from

burning coal at equivalence ratios of 0.5 and 1.1. In view of the above disagreement, a thorough study of PAH emissions over a wide range of equivalence ratios is warranted.

Studies of PAH measurement from combustion of tires, either in tire-to-energy plants or under controlled conditions in laboratory-scale furnaces, are sparse. Most of the studies pertain to tire pyrolysis under inert conditions (see ref 35). Drabek and Willeberg (*36*) measured PAHs from the stacks of two mills using tire chips as a supplement to wood fuel. Their results showed that substitution of a fraction of the wood fuel with tire chips did not significantly increase the emissions of PAHs. Lemieux and Ryan (*37*) examined scrap tire fires and made observations on the emissions from different size cuts. Larger chunks appeared to emit larger quantities of lighter PAHs; however, the evolution of heavier compounds was comparable. Lemieux (*12*) burned wire-free tire chunks (6.4 mm) in a rotary kiln incinerator co-fired with natural gas. With up to 20% tire fuel loading tested, no significant differences from the emissions of plain natural gas were noticed.

The present study was undertaken to assess and compare PAH emissions as well as NO_x, SO_2, and CO emissions from pulverized coal and waste wire-in tire crumb burning under similar well-controlled conditions. The goal was to understand the influence of combustion parameters on toxic emissions. Combustion of clouds of particles (aerosols) of pulverized coal and tires under steady-state/steady-flow conditions took place in electrically-heated drop-tube furnaces, in air, at a gas temperature of 1150 °C. Particle/flame temperatures and combustion durations of single particles were measured pyrometricaly, and the post-flame residence time of the gases was assessed. Emissions were monitored at various fuel mass flow rates that resulted in overall bulk equivalence ratios that differed widely. Experiments were also conducted under pyrolytic conditions (in an inert gas atmosphere) to simulate a worse-case scenario in a pulverized-fuel furnace, i.e., severe oxygen deficiency. Finally, the above results on the emissions from steady flow combustion of particle clouds were contrasted with those from batch combustion of fixed beds of particles in a horizontal muffle furnace. NO_x, SO_2, CO, and PAH emissions are reported from all runs.

Experimental Section

Fuel Properties. The pulverized samples of waste tire particles were produced by cryogenic grinding and were obtained from Midwest Elastomers Inc. The tires were made from styrene-butadiene rubber (SBR). A high volatile bituminous coal (HVAB, PSOC-1451), obtained from the Pittsburgh Coal Bank, was used for comparison. The composition of both the ground tire and coal feeds used in this particular study is given on a moisture-free basis in Table 1. This particular batch of wire-in tire crumb (containing the metalic wires) had higher ash and sulfur content than normally expected (*12*, *38*). The particle size for the two fuels was different in order to match the flame zone and post-combustion residence time in the furnace, as explained at a later section of the paper.

Combustion Observations. Two similar laminar-flow, drop-tube externally heated furnaces (4.8 kW maximum) and a horizontal muffle furnace (1 kW maximum) were used in this study. The details of the furnaces are provided elsewhere (*4*, *39*, *40*), and only a brief description is given here. In the two vertical (drop-tube) furnaces, water-cooled injectors were used to introduce particles to the top of isothermal zones, 25 cm long and 3.5 cm in diameter. One furnace was sealed (*41*), and the effluent from the combustion of clouds of particles (aerosols) was monitored in controlled atmospheres. The other furnace (*42*) incorporated long slotted windows at two diametrically-opposite sides to facilitate cinematographic observations and was coupled to a three-color optical pyrometer (*42*, *43*) through an optical fiber. In this furnace, single particles were burned in air, and their combustion intensity was monitored by the pyrometer along the vertical path of their flight, in the manner of Timothy and Sarofim (*44*) and Levendis and Flagan (*45*). A simplified schematic showing features of both vertical furnaces is depicted in Figure 1. Gas was introduced in these vertical furnaces through the furnace injector and also through a concentric flow straightener, positioned in the annular space between the injector and the alumina tube. The main air flow through the flow straightener was preheated (to about 80% of the final temperature) before it entered the radiation cavity. The gas flow rates in the furnace were adjusted to provide a nominal gas residence time in the isothermal radiation zone of 0.75−1.0 s. Furnace wall temperatures were continuously monitored by type-S thermocouples embedded in the wall. Gas temperatures inside the furnace were measured at various axial and radial positions by an aspirated shielded thermocouple (suction pyrometer) (*46*, *47*). The gas temperature profile along the centerline of the furnace was found to be fairly isothermal, see refs 39 and 47, and gas temperatures were measured to be ≈50 °C lower than the wall temperatures.

TABLE 1
Composition of Fuels

property	ground tire (SBR)	bituminous coal (PSOC-1451)
particle size (μm)	180−212	63−75
fixed carbon (%)	21.7	51.9
volatiles (%)	52.3	34.4
ash (%)	26.0	13.7
carbon (%)	60.9	71.9
hydrogen (%)	5.3	4.7
sulfur (%)	2.46	1.36
nitrogen (%)	0.28	1.36
oxygen (%)	7.1	7.0
heating value (MJ/kg)	29	29.2

Pyrometry and Cinematography. A three-color near-infrared pyrometer was used to obtain the time−temperature histories of burning particles in one of the vertical furnaces. The details of the pyrometer are described in ref 43. Medium bandwidth (70-nm) interference filters were used with wavelengths centered at 0.64, 0.81, and 1.0 μm. Silicon photodetectors were used for recording the radiation in all three channels. The current output was converted to voltage and was then amplified by pre-amplifiers ($\times 10^9$). The time constant of the circuit was less than 1 ms. The signals were converted by a Data Translation (DT2828, 12-bit resolution) A/D high-speed board and were recorded on a IBM-AT (8 MHz, 2.64 MB RAM) personal computer using the Asyst software. A high speed camera was used to record combustion events of single particles or groups of particles at a speed of 200 frames/s, viewing radially through the slotted windows of one of the vertical furnaces.

Batch Combustion in the Horizontal Furnace. Batch combustion experiments involving fixed beds of particles

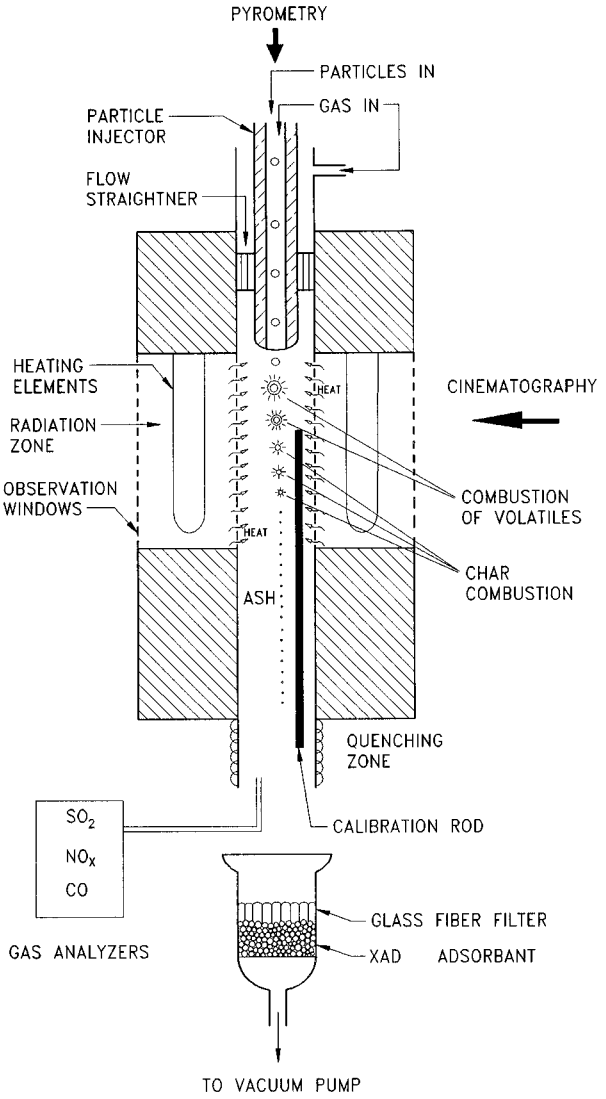

FIGURE 1. General Schematic showing features of the laminar flow furnaces used for the combustion observations as well as for pyrolysis/combustion and emission measurements of dry-injected clouds (aerosols) of particles.

were conducted in a horizontal split-cell furnace fitted with a quartz tube, 4 cm in diameter and 87 cm long, at a wall temperature of 990 °C. The gas temperature profile was measured by the suction pyrometer. The temperature was found to increase axially in the first half of the furnace, but was fairly constant in the second half of the furnace at ca. 950 °C. Thus, the first half length of the furnace acted as an air preheater. Upon reaching the predetermined wall temperature, a porcelain boat loaded with 0.75 g of sample was inserted from the tube's exit, and it was positioned in the middle of the quartz tube. The air flow rate was 5 L/min, and the gas residence time in the second half of the tube (downstream of the sample) was 1 s. Sampling for particulates and hydrocarbons was conducted at the exit of the furnace (*40*).

Emissions Monitoring. *SO_2, NO_x, and CO.* Emissions from the combustion of clouds (well-dispersed aerosols) of ground tires and pulverized coal were measured in the sealed furnace. The powders were pneumatically introduced with the aid of a particle feeding system (*39*, *41*) through the furnace injector. All experiments were conducted in air containing 50 ppm of SO_2, which was introduced to offset the absorbing tendencies of the alumina tube of the furnace (*39*). When saturation was reached and the effluent concentration did not change any longer, the fuel particles were introduced and dispersed in the furnace.

Upon removing moisture with a Permapure dryer, the furnace effluent was monitored for SO_2 using a Rosemount Analytical 590 UV SO_2 analyzer, for NO_x using a Beckman 951A chemilluminescent NO/NO_x analyzer, and for CO using a Beckman 890 infrared analyzer. The analyzer signals were recorded using an Omega analog-to-digital converter interfaced with an IBM AT-286 personal computer running Omega data acquisition software and Lotus 123.

The injection rate of the powders during these experiments was ≈0.14−0.6 g/min, and the total mass flow rate of air was 3.5 g/min. The calculated overall bulk equivalence ratios ϕ varied between 0.5 and 1.8 for both fuels. The bulk equivalence ratio is defined as

$$\phi = \left(\frac{m_{\text{fuel}}}{m_{\text{air}}}\right)_{\text{actual}} \Big/ \left(\frac{m_{\text{fuel}}}{m_{\text{air}}}\right)_{\text{stoichiometric}} \quad (1)$$

The equivalence ratio is equal to the inverse of the excess air ratio, λ.

The signals from the analyzers were recorded for the duration of the tire/coal injection and subsequently were converted to partial pressures. Each experiment lasted between 5 and 15 min. A constant gas flow rate was introduced to the furnace (at STP) resulting in a gas residence time of ≈1 s at T_g = 1150 °C.

Aromatic Hydrocarbon Emissions. Unburned aromatic hydrocarbon emissions from the combustion of clouds of ground tires and pulverized coal were also measured in the sealed furnace. The main parameter of interest in these experiments was the equivalence ratio, ϕ, which was varied from 0.1 to 5 and approached infinity in the pyrolysis runs (in N_2). Experiments were conducted at T_g = 1150 °C. The injection rate of the powders during these particular experiments was varied in the range of 0.07−2.8 g/min, and the total mass flow rate of air was 4.7 g/min; hence, fuel-lean, near-stoichiometric and fuel-rich conditions were achieved ($0.1 < \phi < 5$). Emissions from powders injected in the furnace under pyrolytic conditions (in N_2) were also examined. Finally, combustion of steady-flow injections of particles (aerosols) was contrasted with batch combustion of particles in fixed beds.

Extraction and Concentration of PAH Emissions. Polynuclear aromatic hydrocarbons (PAHs) were monitored at the exit of the furnace by trapping the particulate-(condensed) and gas-phase compounds separately. The sampling stage was placed directly below the furnace (see Figure 1) to minimize losses. Particles (soot, ash, unburned carbon) were trapped on a glass fiber filter. Gas-phase emissions were trapped in a bed of Supelco XAD-4 resin. XAD-4 and the filters were precleaned before use. Precleaning was performed by running in Soxhlet apparatus for two 12-h periods using methylene chloride as the solvent, with changing the solvent between the two periods. All glassware was precleaned with a similar procedure before use. The water bath was maintained at approximately 60 °C during the extraction procedure. The resin and the filters were then air-dried before use.

After the experiments were completed, the used resin and the filters were stored in Teflon-lined jars at 0 °C and were extracted separately by Soxhlet extraction for a 24-h period with methylene chloride, at 60 °C. Before extraction,

100 μg of naphthalene-d_8 was added to the resin as well as to the filter as an internal standard. After extraction, the samples (200 and 300 mL for filter and resin, respectively) were concentrated to a final volume of ≈10 mL using a Büchi rotavapor, at a rate of ≈300 mL/h and a bath temperature of 25 °C and, again, stored in Teflon-lined vials at 0 °C before being analyzed by gas chromatography/mass spectrometry (GC/MS) techniques. The time that elapsed between experiments and GC/MS analysis was always less than 2 weeks.

Mass Spectrometry Analysis. The samples were brought to a final volume of 1 mL and spiked with 100 μg of anthracene-d_{10}. The comparison of the peak areas of the naphthalene-d_8 and anthracene-d_{10} in the total ion chromatogram (TIC) provided a value of extraction efficiency. Experiments were repeated if the extraction efficiency was less than 30%. The data were normalized to the remaining naphthalene-d_8. This procedure enabled a semiquantitation of organic components that appeared in the chromatogram.

The GC/MS system consisted of a Hewlett Packard (HP) Model 5890 Series II GC and an HP Model 5971 mass selective detector. The GC was equipped with an autosampler and tray. The GC column was an HP Ultra-2, 5% phenylmethylsilicone with a length of 25 m, an inside diameter of 0.2 mm, and a film thickness of 0.33 μm. The column head pressure was 480 mbar, the flow rate was 0.7 mL/min, and the linear flow rate was 32 cm/s (methane) at 100 °C. The split flow was 2.0 mL/min, and the split ratio was 2.7:1. The syringe was washed with five 10 μL aliquots of methylene chloride and then washed with two 10-μL aliquots of the sample prior to injection of 1 μL of the analyte. Under these conditions, no ghost peaks resulting from a previous injection were observed. The purge valve was initially closed and was actuated at 0.6 min into the run to remove any remaining volatile materials from the injection port. The injection port temperature was set at 250 °C, the interface was set at 300 °C, and the source was set at 280 °C. The initial oven temperature was 100 °C and was held constant for 4 min before ramping at 4 °C/min to a final oven temperature of 300 °C and holding for 15 min, resulting in a total run time of 68 min. The standard tune files were utilized, and the solvent delay was 3.35 min. The data were collected and processed utilizing Hewlett-Packard Version C.00.07 MS Data Analysis Software and complemented with the 75000 NBS MS full-scan library.

Note that the precise identification and quantitation of every single component of each chromatogram would have required a standard for each compound, and this level of work was considered to be beyond the scope of this research. Components with similar retention times and mass spectral features were often difficult to differentiate, but standards from NIST (Standard Reference Material 159) and the literature were used as guides in establishing the identity of the components. The comparative analysis of the condensed phase (soot, ash, unburned fuel) collected on the filter and the gas phase, adsorbed on the XAD-4 resin, showed that most of the semivolatile components observed on the filter paper extracts were also observed in the XAD-4 resin extracts. Occasionally at high equivalence ratios, traces of fine soot particles leaked around the filter and found their way to the XAD-4 bed; thus, the gas-phase analysis may contain traces of the solid phase PAHs.

To identify and semiquantify interferences resulting from the test facility, i.e., the furnace, filter paper, XAD-4 resin, solvents, and GC/MS instrumentation, a combustion blank experiment was devised: the experimental procedure was followed exactly, omitting only the fluidization and combustion of polymer particles. Compounds such as xylenes (from the XAD-4), siloxanes (from the GC column or the apparatus), and bis(2-ethylhexyl) phthalate were not included in the sample data because they were observed in large quantities in the blank experiment. Note, however, that it would have been unwise to subtract the amount of these compounds observed in the blank experiment without incorporating sufficient replicate analysis. Laboratory blank experiments were also conducted by extracting precleaned XAD-4.

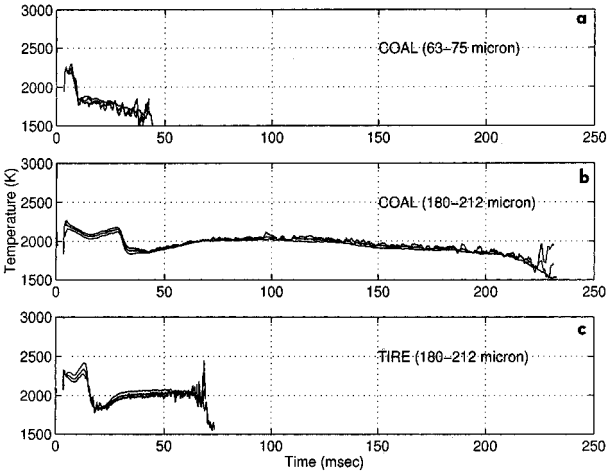

FIGURE 2. Three-color temperature−time histories for three different coal and tire particles burning in air at $T_g \approx 1150$ °C; (a) coal particle 63−75 μm, (b) coal particle 180−212 μm, and (c) tire particle 180−212 μm.

All test parameters used in these experiments (the flow rates, pressures, temperatures, amounts of XAD-4, extraction, and chromatographic conditions) were kept constant in all tests. One combustion test was conducted at each ϕ. The reason was that fluidization of the fuel powder could not be precisely controlled. Small variations in the fluidization resulted in a different equivalence ratio, ϕ. Three successful repeats were accomplished burning tire crumb at a ϕ of 1.75. Results showed a standard deviation of 14% for the total amount of PAHs detected and under 20% for most individual components, but in this region even small variations in ϕ can cause large variations in PAH emissions (it is the onset of the exponential behavior that will be shown later in Figures 8 and 9).

Results and Discussion

Particle Combustion. Combustion of individual particles of coal and tire rubber was monitored pyrometricaly and cinematographically. Detailed results on single particle combustion have been presented elsewhere (*4*). Experiments were also conducted for the particle sizes of the present study and typical results are shown in Figures 2 and 3. Pyrometricaly-obtained temperature profiles (*43*) for three single particles are shown in Figure 2. The superimposed profiles correspond to the three two-color temperatures deduced from the radiation signals captured by the three-wavelength pyrometer. Temperatures were derived based on the gray radiation assumption, i.e., the emissivity was assumed to be independent of the wavelength of observation. The initial hump in each profile corresponds to evolving volatiles burning in envelope

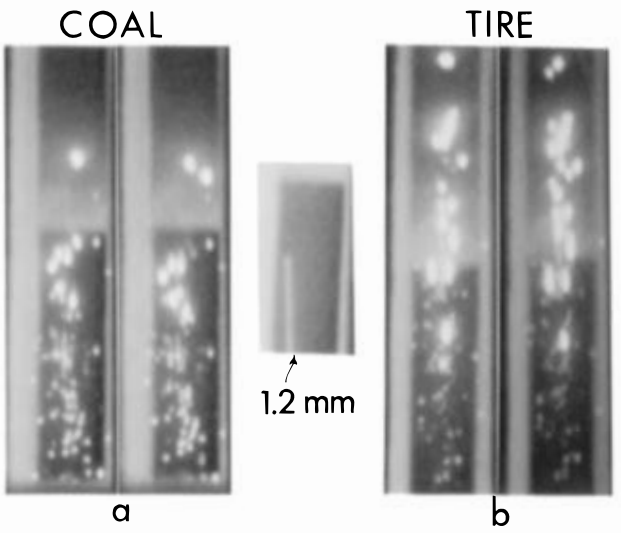

FIGURE 3. Selected frames from high-speed cinematography (spaced 5 ms apart) of dry-injected particles burning as aerosols, in air at $T_g \approx 1150$ °C; (a) coal and (b) tire particles (180−212 μm) corresponding to an overall ϕ of 1.0.The calibration rod, shown inserted in the furnace, had a diameter of 1.2 mm.

flames. The first two cases depict coal particles in the size ranges of 63−75 μm and 180−212 μm, Figure 2a,b, respectively. The third case depicts a burning tire particle in the size range of 180−212 μm. Maximum flame temperatures reached 2250 K, and char temperatures were 2000 K or below. Overall particle combustion durations were less than one-fourth of a second. It is worth noticing, by contrasting Figure 2b,c, that for similar size coal and tire particles the combustion of the latter was much briefer (by a factor of 3), which can be partially attributed to their lower density (0.47 and 1.18 g/cm^3 for tire and coal, respectively) and to their higher volatile fraction.

Examples of combustion of steady-flow clouds of coal and tire particles (180−212 μm) are shown in Figure 3. Combustion took place in air at a bulk equivalence ratio around 1.0. Notice the large bright flames during the volatile combustion phase, followed by the dimmer char combustion phase.

Useful data on the post-flame residence times in the furnace are also gathered from such photographs since the length of the particle combustion zone in the furnace can be directly observed. Thus subtracting the ignition and combustion lengths from the total length of the furnace, the length of the post-combustion zone can be measured. Based on the known flow rates, the post-combustion residence times are thus inferred. For instance, in the case of Figure 3b, particle combustion occurs in the middle height of the furnace; thus, only a fraction of the given nominal residence time is actually available for post-combustion reactions in this particular case (tire particles 180−212 μm). Other cases vary according to the particle type and size, temperature, and ϕ, and adverse conditions (high ϕ, low gas temperature, and large particle size) may stretch the combustion zone to the bottom of the furnace. Thus, for all cases reported herein, the actual post-flame residence time of the combustion products was always less than the aforementioned nominal times of 0.75−1.0 s.

NO_x, SO_2, and CO Emissions. Emissions from the combustion of steady-state/steady-flow clouds of particles (aerosols) in the vertical furnace (VF) are listed in Table 2,

TABLE 2

NO_x, SO_2, and CO Emissions from Combustion of Steady-State/Steady-Flow Groups of Particles in Drop-Tube Furnace, at $T_g = 1150$ °C

fuel	ϕ	NO_x (ppm, mg of NO/ g of fuel, wt % fuel N)	SO_2 (ppm, mg of SO_2/ g of fuel, wt % fuel S)	CO (%, mg of CO/ g of fuel, wt % fuel C)
coal	0.7	809, 13.0, 35	688, 20.1, 74	0.02, 3, 0.1
	1.0	806, 8.4, 23	754, 16.8, 62	0.05, 5.3, 0.3
	1.5	543, 5.4, 15	875, 18.0, 66	0.68, 62.5, 2.4
tire	0.6	205, 3.7, 42	916, 34.6, 70	0.01, 1.8, 0.1
	1.0	302, 3.6, 43	1340, 35.0, 71	0.07, 8.9, 0.6
	1.8	177, 1.3, 15	1940, 31.4, 64	0.85, 59.9, 4.2

under fuel-lean, stoichiometric, and fuel-rich conditions. The reported equivalence ratio corresponds to an overall bulk condition of the particle clouds. While knowledge of such a bulk ϕ is of little consequence for characterizing local conditions inside and outside diffusion envelope particle flames during the combustion of volatiles, it becomes meaningful for the char combustion phase as well as useful in assessing the availability of oxygen in the post-combustion zone. The entries in Table 2 represent the emissions in partial pressures in the effluent gas as well as in milligram per gram of fuel burned, i.e., after the combustion efficiency was accounted for. Thus

$$\dot{m}_{\text{fuel burned}} = \eta_f[(\dot{m}_{\text{fuel supplied}} - \dot{m}_{\text{ash}})\eta_{\text{combustion}} + \dot{m}_{\text{ash}}]$$

where η_f is the fluidization efficiency, which accounts for particle losses in the delivery tubing (set equal to 95%), $\eta_{\text{combustion}}$ was measured from ashing of the solid residue collected at the bottom of the furnace.

NO_x (NO + NO_2) emissions of tires were much lower than those of coal (by a factor of 3), reflecting their lower nitrogen content. The nitrogen content of the tire crumb burned herein is equal to a typical average nitrogen content of tires, i.e., 0.29% (*38*). As the equivalence ratio increased, the partial pressure of NO_x initially increased because of higher fuel loading and then decreased as stoichiometry was approached or exceeded because of limited oxygen availability (*48*). When these results were expressed in (mg of NO)/(g of fuel burned), the emissions dropped drastically with ϕ throughout the range examined [for these calculations all NO_x was expressed as NO since this is the predominant component (*48*)]. This trend indeed shows that at the conditions of the primary fuel-rich region of low-NO_x burners the formation of NO_x is suppressed. The last entry of this column lists the percentage of the parent nitrogen that was converted to NO_x. This calculation was made with the assumption that roughly 80% and 70% of the detected NO_x originated from the fuel nitrogen content of the coal and tire, respectively (*48*). Based on these assumptions and the values shown in Table 1, an elemental closure on fuel nitrogen was performed. Thus, for coal at ϕ values of 0.8 and 1, 35% and 23%, respectively, of the fuel nitrogen was converted to NO_x, which is comparable to what other investigators reported, see refs 16 and 17. At a ϕ of 1.5, this value dropped to 15%. Most of the remaining fuel nitrogen is expected to have converted to N_2 (*16*), even if some of the intermediate species (HCN, NH_3) may still be present. For tires, the calculations show that a higher fraction of the fuel nitrogen is converted to NO_x than in the

TABLE 3

PAH Detected As Coal Combustion Byproducts (in μg/g of coal) at 0.75 s Nominal Residence Time from XAD-4[a]

gas temp (°C)	1150	1150	1150	1150	1150	1150	1150	1250	1150	1150	950
equivalence ratio	$\phi \sim 0.1$	$\phi \sim 0.3$	$\phi \sim 0.6$	$\phi \sim 1.0$	$\phi \sim 1.2$	$\phi \sim 1.8$	$\phi \sim 2.1$	$\phi \sim 2.4$	$\phi \sim 4.63$		
furnace, gas	VF, air	VF, air	VF, air	VF, air	VF, air	VF, air	VF, air	VF, air	VF, air	VF, N_2	HF, air
PAHs											
naphthalene	2.1	2.0		16.4	112.3	18.8	31.8	162.4	744.4	1804.3	153.6
benzothiophene										125.2	
2-methylnaphthalene										42.2	
1-methylnaphthalene										31.0	
biphenyl										35.2	2.9
acenaphthylene						14.2	41.0	151.0	733.7	1914.5	19.7
acenaphthene						22.0					
dibenzofuran										70.0	4.5
fluorene									25.3	97.2	4.4
dibenzothiophene								5.9	28.1	42.8	7.0
phenanthrene							4.6	53.8	307.6	492.0	28.8
anthracene								7.8	61.2	140.4	6.3
3-methylphenanthrene											
2-methylphenanthrene											
4-*H*-cyclopenta[*def*]phenanthrene								14.7	103.9	123.6	14.0
fluoranthene						12.0	34.7	91.7	1136.6	692.2	28.7
acephenanthrylene								19.6	293.1	234.8	14.3
phenanthro[4,5-*bcd*]thiophene								8.5	65.1	41.3	26.8
pyrene						22.9	62.9	96.6	1153.7	653.2	25.1
benzo[*a*]fluorene									17.9	44.3	
benzo[*b*]fluorene									16.7	17.7	
1-methylpyrene										49.1	
benzo[*b*]naphthol[2.1-*d*]thiophene											
benzo[*ghi*]fluoranthene								16.4	260.0	25.9	
benzo[*c*]phenanthrene								6.1		120.6	
benzo[*b*]naphthol[2,3-*d*]thiophene										56.4	
cyclopenta[*cd*]pyrene								54.0	1142.9	413.2	40.3
benz[*a*]anthracene								7.3	0.8	40.4	16.8
chrysene/triphenylene										78.8	
benzo[*b*]fluoranthene								9.2	157.1	57.0	
benzo[*j*]fluoranthene										29.0	
benzo[*a*]fluoranthene									66.5	15.1	
benzo[*e*]pyrene								4.6		22.8	
benzo[*a*]pyrene								9.2	59.4	50.6	
perylene									13.5	19.9	
total in mg/g	0.00	0.00	0.00	0.02	0.11	0.09	0.18	0.72	6.39	7.58	0.39
total in mg/g (exc. naphthalene)	0.00	0.00	0.00	0.00	0.00	0.07	0.14	0.56	5.64	5.78	0.24

[a] Blank values indicate that less than 1 μg/g of coal was observed. VF, vertical furnace; HF, horizontal furnace.

case of coal. This may be partly attributed to the fact that most of the combustible mass of tire particles is volatile and burns in diffusion flames at high temperature and with adequate supplies of oxygen, hence, forming NO. To the contrary, most of the mass of coal is fixed carbon and burns heterogeneously in the diffusion-controlled regime III, i.e., at very low surface oxygen concentration and minimal penetration in the pores. Thus, the reducing atmosphere inside the chars favors the formation of N_2 instead of NO (*16*).

Combustion of this particular batch of tire crumb generated higher SO_2 emissions than the bituminous coal examined. This is not surprizing since the SO_2 emissions are proportional to the sulfur content of fuels, and this tire sample contained 1.8 times more sulfur than coal (see Table 1). This is unusual however since the average sulfur content of tires is 1.57% (*38*). Indeed, another sample obtained from the same supplier contained 1.7% sulfur (*22*, *49*). The partial pressure of SO_2 in the effluent increased with the equivalence ratio because of the higher fuel loading in the combustion chamber. However, the specific SO_2 emissions in (mg of SO_2)/(g of fuel burned) showed little variation with the equivalence ratio, indicating only a mild dependence on the oxygen concentration. An elemental balance on the sulfur shows that most of the sulfur converted to SO_2. A total of 5−6% of the initial sulfur content of tire crumb was found in the ash (*49*). Other species, such as H_2S, elemental S, SO_3, etc. may account for the difference.

CO emissions from tire and coal were rather low (0.01−0.03 mol %), in the fuel-lean region ($\phi = 0.6-0.7$) (see Table 2). The corresponding combustion efficiencies as deduced from ashing experiments (*48*) were 98% and 99% for tire and coal, respectively. At stoichiometry, combustion efficiencies dropped to 89 and 86%, but CO concentrations remained relatively low at 0.05−0.07%. In the fuel-rich region ($\phi = 1.3-1.8$), the combustion efficiencies dropped further to 80% and 76% for tire and coal, but the CO emissions increased dramatically to 0.85 and 0.68% for tire and coal, respectively. This signifies that a small percentage of the carbon content in the fuel was converted to CO (see Table 2) because of oxygen deficiency.

Gas-Phase PAH Emissions. The predominant PAHs (EPA list) that were detected in both the gas-phase effluent (on XAD-4) and in the solid phase (on filters) during combustion/pyrolysis experiments with pulverized coal and tire, are listed in Tables 3−7. Results from combustion experiments of steady-flow clouds of particles in the vertical furnace (VF), at ϕ values ranging from 0.1 to 5, in air are

TABLE 4

PAH Detected as Tire Crumb Combustion Byproducts (in μg/g of tire) at 0.75 s Nominal Residence Time from XAD-4[a]

gas temp (°C)	1150	1150	1150	1150	1150	1150	1150	1150	1150	1150	950
equivalence ratio	$\phi \sim 0.1$	$\phi \sim 0.3$	$\phi \sim 0.6$	$\phi \sim 0.8$	$\phi \sim 1.5$	$\phi \sim 1.7$	$\phi \sim 1.9$	$\phi \sim 2.3$	$\phi \sim 5.0$		
furnace, gas	VF, air	VF, air	VF, air	VF, air	VF, air	VF, air	VF, air	VF, air	VF, air	VF, N_2	HF, air
PAHs											
naphthalene	44.1	5.7	34.0	30.5	221.4	127.3	442.7	627.6	1008.9	5691.9	1224.7
benzothiophene					36.3	10.1		42.7		847.8	4.5
2-methylnaphthalene							5.7			436.8	744.1
1-methylnaphthalene							2.9			354.9	48.3
biphenyl					3.8		11.7	21.2	50.4	667.8	266.0
acenaphthylene			15.5	13.8	139.3	148.7	295.5	385.7	792.5	4400.0	656.5
acenaphthene							8.4		22.9		
dibenzofuran									4.4		
fluorene							8.7	12.5	27.6	635.1	144.1
dibenzothiophene					8.1		14.0	27.3	84.8	249.2	30.1
phenanthrene			4.6	4.1	49.0	57.8	81.5	170.3	702.9	1764.9	753.2
anthracene					7.8		10.0	10.8	47.1	481.9	23.2
3-methylphenanthrene										73.2	9.3
2-methylphenanthrene										69.5	9.1
4-*H*-cyclopenta[*def*]phenanthrene					11.4		13.4	19.7	62.3	484.9	88.5
fluoranthene			5.3	6.8	76.3	122.3	96.4	136.5	989.7	1145.9	338.8
acephenanthrylene					19.9	22.9	24.8	29.3	222.9	552.7	126.1
phenanthro[4,5-*bcd*]thiophene					16.7	23.6	19.5	19.7	157.3	126.2	12.3
pyrene			4.1	6.7	92.3	142.3	104.1	122.4	1074.8	1041.6	327.1
benzo[*a*]fluorene									14.5	251.9	32.0
benzo[*b*]fluorene									16.3	261.1	35.3
1-methylpyrene									13.8	160.3	32.4
benzo[*b*]naphthol[2,1-*d*]thiophene							2.3		25.2	138.1	15.2
benzo[*ghi*]fluoranthene					18.8	32.7	20.4	33.2	212.2	266.5	60.8
benzo[*c*]phenanthrene					4.7		4.7			129.7	22.0
benzo[*b*]naphthol[2,3-*d*]thiophene							3.0			78.9	
cyclopenta[*cd*]pyrene					55.1	60.0	46.3	116.4	726.7	731.6	156.3
benz[*a*]anthracene					15.7		6.0		112.4	258.6	75.9
chrysene/triphenylene						20.8	15.0	12.1	280.1	200.0	
benzo[*b*]fluoranthene					5.5		8.0		169.7	259.7	60.0
benzo[*j*]fluoranthene							6.6	17.1	5.6	123.8	26.0
benzo[*a*]fluoranthene							8.2	59.6			
benzo[*e*]pyrene					2.1		8.3	8.4	114.4	123.0	18.5
benzo[*a*]pyrene					2.2		8.3		122.4	154.6	35.7
perylene									51.4	95.1	12.8
total in mg/g	0.04	0.01	0.06	0.06	0.79	0.77	1.27	1.82	7.17	22.26	5.39
total in mg/g (exc. naphthalene)	0.00	0.00	0.03	0.03	0.57	0.64	0.83	1.19	6.16	16.57	4.16

[a] Blank values indicate that less than 1 μg/g of tire was observed. VF, vertical furnace; HF, horizontal furnace.

TABLE 5

Relative Gas-Phase Emissions (Tire/Coal) of Selected PAHs

PAH	pyrolysis, N_2, VF	aerosol comb. air, VF		fixed bed comb., air, HF, air, HF
		$\phi \approx 5$	$\phi \approx 2.3$	
phenanthrene	3.6	2.3	3.2	27
pyrene	1.6	0.9	1.3	13.6
fluoranthene	1.7	0.9	1.5	12.1
acephenanthrylene	2.3	0.8	1.5	9.4
benzo[*ghi*]fluoranthene	10.8	0.8	2.0	>45
cyclopenta[*cd*]pyrene	1.8	0.6	2.1	>117
benzo[*a*]pyrene	3.0	2.0		>27

included. Results from batch experiments, involving combustion of fixed beds of particles in air, in the horizontal furnace (HF) are also included. In this section, specific PAH emissions are expressed per mass of fuel introduced in the furnace and not per mass of fuel actually burned, as was done earlier for the cases shown in Table 2. The main reason for this difference is that ashing experiments could not be performed herein to obtain the combustion efficiency, since the residue was used for Soxhlet extraction. An example of a total ion chromatogram from a combustion experiment is shown in Figure 4.

A review of the gas-phase PAH yields (i.e., the emissions trapped in the XAD-4 resin) from the experiments involving steady-state combustion of clouds of particles (aerosols) in the vertical drop-tube furnace reveals the following:

Pyrolysis. Under pyrolytic conditions in N_2 at $T_g = 1150$ °C and a gas residence time of 0.75 s, both fuels emitted the highest total amounts of PAHs as well as the highest amount of most individual PAHs (see Tables 3 and 4). Individual PAH emissions from pulverized tires exceeded those of coal typically by a factor of 1.6−3.6, with benzo[*ghi*]fluoranthene emitted 11 times more (see Table 5). The total amount of PAHs emitted per gram of coal fed was 7.58 mg, while that emitted per gram of tire crumb was 22.26 mg. Thus, cumulative PAH emissions from the pyrolysis of pulverized tires exceeded those of pulverized coal by a factor of 3. The highest concentration PAH components in the effluent are shown in Figure 5. The compounds shown in Figure 5 are highly fused structures and resulted primarily from the pyrolysis process. The larger four-ring structures of pyrene and the five-ring structures, such as

TABLE 6

PAH Detected as Coal Combustion Byproducts (in μg/g of coal) at 0.75 s Nominal Residence Time from Ash and Soot Collected on Filter Paper[a]

gas temp (°C)	1150	1150	1150	1150	1150	1150	1150	1250	1150	1150	950
equivalence ratio	$\phi \sim 0.1$	$\phi \sim 0.3$	$\phi \sim 0.6$	$\phi \sim 1.0$	$\phi \sim 1.2$	$\phi \sim 1.8$	$\phi \sim 2.1$	$\phi \sim 2.4$	$\phi \sim 4.6$		
furnace, gas	VF, air	VF, air	VF, air	VF, air	VF, air	VF, air	VF, air	VF, air	VF, air	VF, N_2	HF, air
PAHs											
naphthalene						36.0	96.6	157.9		17.8	11.3
benzothiophene											
2-methylnaphthalene											
1-methylnaphthalene											
biphenyl											
acenaphthylene						47.9	174.1	275.2	358.6	183.6	
acenaphthene											
dibenzofuran											
fluorene										16.2	
dibenzothiophene								22.3		15.9	
phenanthrene							50.6	28.6	527.3	68.7	9.7
anthracene								4.0		24.1	
3-methylphenanthrene											
2-methylphenanthrene											
4-*H*-cyclopenta[*def*]phenanthrene								39.7	76.3	33.6	
fluoranthene							174.1	221.1	1321.0	167.6	
acephenanthrylene							22.4	33.8	274.9	40.4	
phenanthro[4,5-*bcd*]thiophene							26.9	40.5	115.9	44.0	
pyrene						27.0	302.8	157.7	1598.0	95.4	
benzo[*a*]fluorene											
benzo[*b*]fluorene											
1-methylpyrene											
benzo[*b*]naphtho[2,1-*d*]thiophene											
benzo[*ghi*]fluoranthene								38.3	218.6	24.7	
benzo[*c*]phenanthrene									77.8		
benzo[*b*]naphthol[2,3-*d*]thiophene											
cyclopenta[*cd*]pyrene								108.0	890.1	91.1	
benz[*a*]anthracene											
chrysene/triphenylene										17.3	
benzo[*b*]fluoranthene										22.7	
benzo[*j*]fluoranthene										12.5	
benzo[*a*]fluoranthene										13.6	
benzo[*e*]pyrene										20.5	
benzo[*a*]pyrene											
perylene											
total in mg/g						0.11	0.85	1.13	5.46	0.91	0.02
total in mg/g (exc. naphthalene)						0.07	0.75	0.97	5.46	0.89	0.01

[a] Blank values indicate that less than 1 μg/g of coal was observed. VF, vertical furnace; HF, horizontal furnace.

perylene, are likely to be flash-vaporized from the surface of coal/tire and survive the pyrolysis process.

Combustion. When at the same temperature and gas residence time as above, oxygen was introduced in the furnace to achieve an overall ϕ in the vicinity of 5, i.e., extremely fuel-rich conditions, the concentration of most PAHs was reduced. For coal, a few of the PAHs, such as fluoranthene, pyrene, and cyclopenta[*cd*]pyrene, showed an increase in concentration (by a factor of 2) when oxygen was introduced, but most PAHs decreased, and the total amounts were 7.58 mg/(g of coal) in N_2 and 6.39 mg/(g of coal) in the presence of O_2 at $\phi = 4.6$ (see Table 3). For tire, the concentration of nearly all PAH components was reduced in the presence of oxygen, and the total amounts were 22.26 mg/(g of tire) in N_2 and 7.17 mg/(g of tire) at $\phi = 5.0$ (see Table 4). When more oxygen was introduced and ϕ was reduced in the neighborhood of 2, the concentrations of PAHs were further reduced by as much as an order of magnitude. For example, at $\phi \approx 2.3$, the total PAH emissions were 1.82 mg/g for tire and 0.72 mg/g for coal. When additional oxygen was introduced, the PAH emissions diminished. For coal, PAHs emissions were hardly detected at equivalence ratios below 1.8 (with the exception of naphthalene). For tire crumb, PAHs could not be detected at $\phi < 0.6$. Moreover, only small amounts of a limited number of PAHs (naphthalene, acenapthylene, phenanthrene, fluoranthene, and pyrene) were present in the effluent of tire crumb in the vicinity of the stoichiometric point. These trends are shown in Tables 3 and 4 and Figure 6 (pulverized coal) and Figure 7 (pulverized tire), where the total ion chromatograms are plotted for different ϕ values as well as in Figures 8 and 9. The fact that PAHs were not present in the effluent of burning fuel-lean and stoichiometric aerosols of coal is in agreement with results reported by Longwell (*30*) concerning nonquenched, premixed flames of hydrocarbon fuels at $\phi <= 1$.

It is interesting to note that while PAH emissions from combustion of tire crumb commenced at a lower ϕ than coal, at severely fuel-rich conditions PAH emissions from both fuels were comparable (see Table 5). This was not the case, however, for batch combustion of fixed beds of particles in the horizontal furnace (HF). Even if the sample size therein was small, 0.75 g of powder, PAH emissions from coal and tire were drastically different. The total as well as the individual PAH amounts from tires were substantially lower than those emitted under pyrolytic conditions and were somewhat lower than those emitted from steady flow combustion of aerosols at $\phi = 5$. Batch

TABLE 7

PAHs Detected as Tire Crumb Combustion Byproducts (in μg/g of tire) at 0.75 s Nominal Residence Time from Ash and Soot Collected on Filter Paper[a]

gas temp (°C)	1150	1150	1150	1150	1150	1150	1150	1150	1150	1150	1150
equivalence ratio	$\phi \sim 0.1$	$\phi \sim 0.3$	$\phi \sim 0.6$	$\phi \sim 0.8$	$\phi \sim 1.5$	$\phi \sim 1.7$	$\phi \sim 1.9$	$\phi \sim 2.3$	$\phi \sim 5.0$		
furnace, gas	VF, air	VF, air	VF, air	VF, air	VF, air	VF, air	VF, air	VF, air	VF, air	VF, N_2	HF, air
PAHs											
naphthalene					160.8	71.6	151.4	244.5	318.1	457.7	53.6
benzothiophene					24.7		23.7	19.8	20.7	41.2	
2-methylnaphthalene										18.6	7.3
1-methylnaphthalene										33.8	6.1
biphenyl								9.8		30.2	135.4
acenaphthylene					133.2	126.0	163.2	219.5	424.8	258.8	572.4
acenaphthene											3.4
dibenzofuran											
fluorene					5.6		4.8			49.3	162.0
dibenzothiophene					6.9		16.1	18.9	49.9	12.9	
phenanthrene					36.2	47.5	58.3	121.1	418.2	85.8	403.4
anthracene							7.2			28.5	115.0
3-methylphenanthrene											9.6
2-methylphenanthrene											13.6
4-*H*-cyclopenta[*def*]phenanthrene					6.5		9.6	8.5	38.4	18.7	100.7
fluoranthene					48.4	89.1	54.4	95.0	718.7	41.2	488.5
acephenanthrylene					9.2		12.0	17.1	144.2	11.6	187.1
phenanthro[4,5-*bcd*]thiophene					11.0		10.8	13.2	114.0	4.9	16.2
pyrene					48.8	104.0	54.1	81.0	781.2	30.7	473.9
benzo[*a*]lfluorene											41.4
benzo[*b*]fluorene											35.5
1-methylpyrene											42.8
benzo[*b*]naphthol[2,1-*d*]thiophene											
benzo[*ghi*]fluoranthene					7.2		11.0	18.3	161.2	12.1	87.9
benzo[*c*]phenanthrene									38.7		29.5
benzo[*b*]naphthol[2,3-*d*]thiophene											
cyclopenta[*cd*]pyrene					12.9		14.7	42.2	472.4	7.5	216.2
benz[*a*]anthracene									79.2		49.8
chrysene/triphenylene					8.4		13.2	9.5	228.7		106.9
benzo[*b*]fluoranthene									106.4		82.2
benzo[*j*]fluoranthene									21.6		33.7
benzo[*a*]fluoranthene									59.7		24.6
benzo[*e*]pyrene									63.4		49.9
benzo[*a*]pyrene									21.1		16.4
perylene											
total in mg/g	0.00	0.00	0.00	0.00	0.52	0.44	0.60	0.92	4.28	1.14	3.56
total in mg/g (exc. naphthalene)	0.00	0.00	0.00	0.00	0.36	0.37	0.45	0.67	3.96	0.69	3.51

[a] Blank values indicate that less than 1 μg/g of tire was observed. VF, vertical furnace; HF, horizontal furnace.

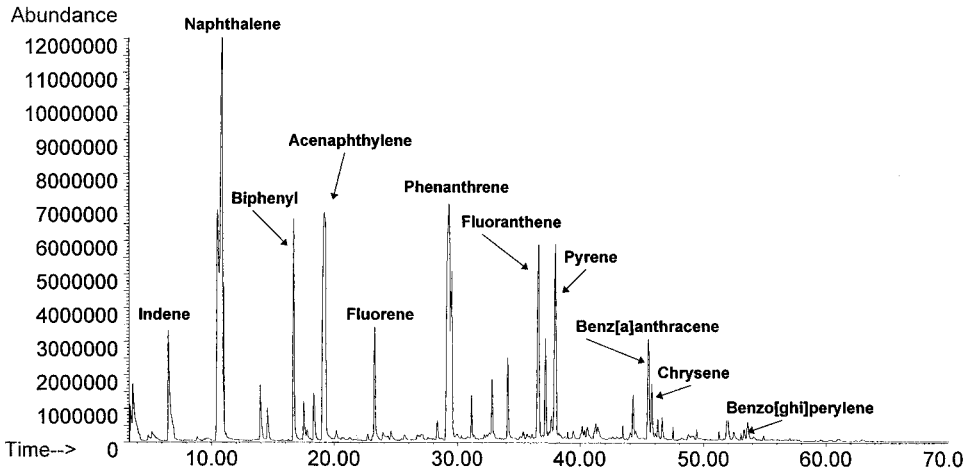

FIGURE 4. Total ion chromatogram showing major gas-phase PAH peaks resulting from combustion of waste tire crumb in horizontal furnace, in air at $T_g \approx 950$ °C.

combustion of coal produced rather low PAH concentrations, comparable to the combustion of its aerosol at $\phi \approx 2.4$. While the emissions from the steady-flow combustion in the vertical furnace and the batch combustion in the horizontal furnace are not exactly comparable, because the mixing conditions in the latter are ill-defined, an overall trend becomes obvious. PAH emissions from the fixed bed combustion of tires were 1−2 orders of magnitude more severe than those of coal under identical conditions. Generally, the types of PAHs produced from the batch

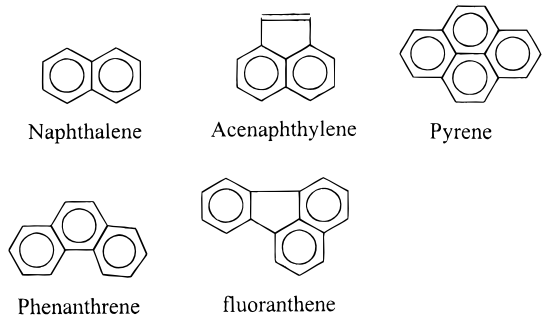

FIGURE 5. Chemical structure of abundantly occurring PAH components in the effluent.

combustion of fixed beds as well as pyrolysis and combustion of clouds of particles varied only in their amounts, but rarely varied in identity.

From the above discussion, it can be concluded that the toxic organic emissions of both fuels are strong functions of the equivalence ratio; in fuel-lean mixtures, PAHs can be effectively destroyed in the combustion and post-flame zones. In fuel-rich mixtures, the emission of PAHs rapidly increases with ϕ and eventually plateaus, asymptotically approaching the emissions under pyrolytic conditions. The onset of significant PAH concentrations with increasing ϕ occurs at substantially higher ϕ for coal ($\phi = 1.5-1.8$) than for tire crumb ($\phi = 0.6-0.8$). The sample size and mixing with air also appeared to be extremely important for tire, but much less so for coal. Tires appeared to burn much "cleaner" when pulverized and injected in a furnace than when combusted in fixed beds (containing either multilayers of small particles or larger chunks) (see Table 4). The mode of burning of coal (fixed beds vs particle clouds) did not appear to influence PAH emissions of coal as much as those of tire (see Table 3). Hence, dry-injection and combustion of tires in pulverized form, if possible, is recommended. This is in complete agreement with the combustion observations outlined earlier and discussed in ref 4. Combustion of large pieces of tires or fixed beds of tire particles generated copious quantities of acrid smoke. To the contrary, no smoke was detected to escape the envelope flame around individual tire particles (up to a size of 220 μm examined herein) or to remain in the furnace upon extinction of the volatile flame (*4*) in contrast to the case of burning polystyrene particles (*50*). This different combustion behavior of tires and coal (i.e., bulk combustion vs aerosol) may be explained on the basis of the large volatile content of tires. For the specific fuels examined herein, tire contained almost twice as much volatile mass per unit weight than coal. Thus, the resulting higher volatile fluxes from tire samples readily created diffusion-limited and locally pyrolytic conditions that favored the generation of condensed species, such as PAHs and soot. Furthermore, TGA experiments reported in ref 4 revealed that evolution of volatiles from tire commences at lower temperatures (200 °C) than from coal (300 °C). Hence, tire pyrolysis may happen more readily, enhancing the formation of PAHs.

A few additional comments concerning the emissions of gas-phase PAHs from coal and tire are as follows: benzo[*a*]pyrene, cyclopenta[*cd*]pyrene, and fluoranthene, among others, are known to exhibit high mutagenic activities (*51*). Within the same sample, the following were found: (a) The concentrations of naphthalene and acenaphthylene were comparable, with the latter assuming lesser values, in agreement with results reported by Longwell for premixed flames (*30*). (b) The concentrations of phenanthrene, fluoranthene, and pyrene were comparable to each other and were less than that of naphthalene. The striking analogy of concentrations of the isomers of pyrene and fluoranthene ($C_{16}H_{10}$) has also been reported by Longwell (*30*) for toluene and acetylene flat flames as well as diesel engines and gasoline engines; however, absolute concentrations varied widely among the different fuels. (c) The concentration of cylopenta[*cd*]pyrene was lower, by up to a factor of 2, than that of pyrene, except in the case of batch combustion of coal. (d) The concentration of benzo[*a*]pyrene was lower than cyclopenta[*cd*]pyrene by an additional factor of 5. Given the completely different nature of the fuels herein as well as those discussed by Longwell (*30*), such similarities are notable and may indicate PAH growth by a similar mechanism.

Relationship of ϕ to Gas-Phase PAH Emissions. In the steady-flow aerosol combustion in the VF, the equivalence

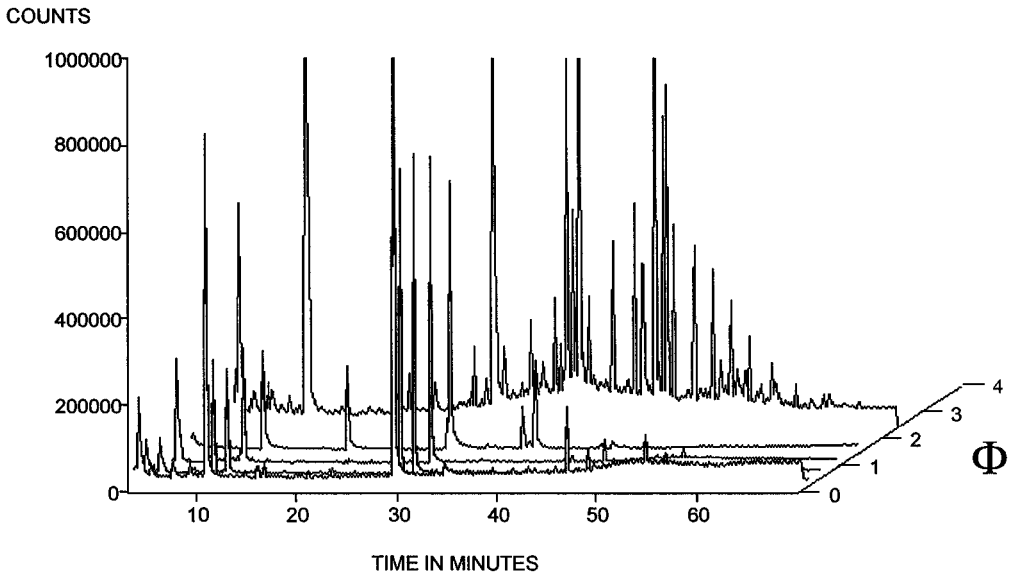

FIGURE 6. Superimposed total ion chromatograms of gas-phase PAHs for different values of ϕ from combustion of aerosols of pulverized coal in the vertical furnace at $T_g \approx 1150$ °C.

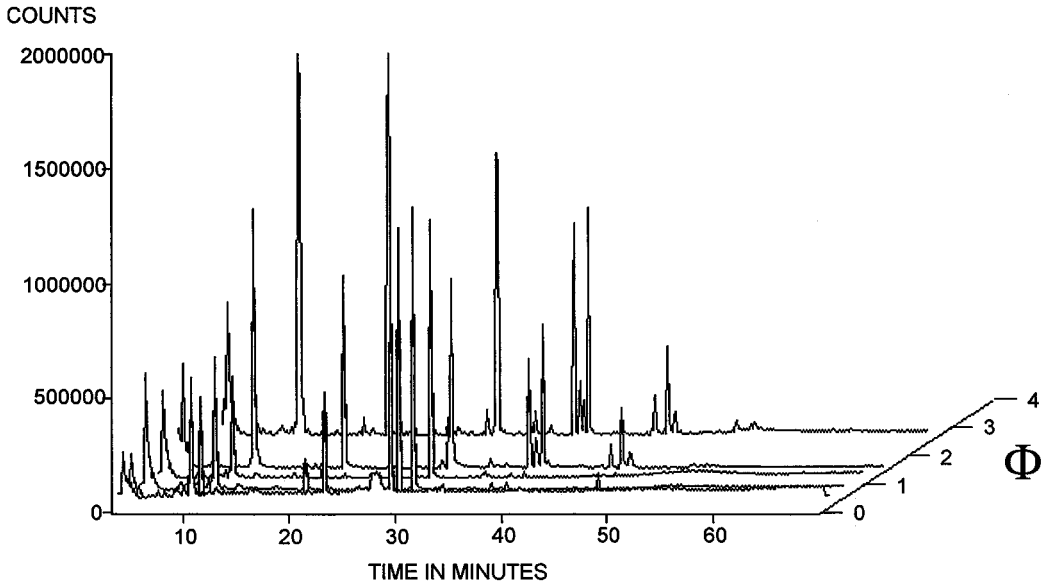

FIGURE 7. Superimposed total ion chromatograms of gas-phase PAHs for different values of ϕ from combustion of aerosols of tire crumb in the vertical furnace at $T_g \approx 1150$ °C.

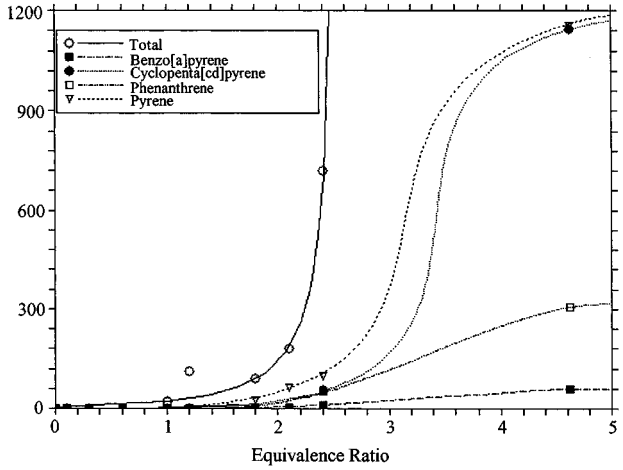

FIGURE 8. Variation of individual gas-phase PAHs (in μg/g of coal combusted) as well as total amounts with ϕ, resulting from combustion of aerosols of pulverized coal in the vertical furnace at a $T_g \approx 1150$ °C.

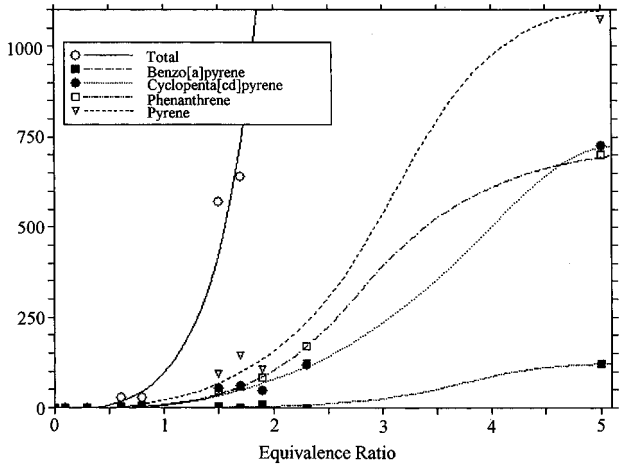

FIGURE 9. Variation of individual gas-phase PAHs (in μg/g of coal combusted) as well as total amounts with ϕ, resulting from combustion of aerosols of tire crumb in the vertical furnace at a $T_g \approx 1150$ °C.

ratio ϕ was varied at a constant gas temperature of 1150 °C. At a ϕ of 1.0, small amounts of PAHs were detected from the combustion of pulverized tire and even less from that of coal. As ϕ was reduced, increasingly smaller amounts of PAHs were detected until a ϕ value of 0.6, after which point no PAHs were detected from either fuel. Thus, PAH production exhibited an asymptotic behavior as ϕ approached zero. At ϕ values greater than 1.0, the amount of PAHs detected increased exponentially with ϕ. However, since at the most extreme fuel-rich conditions explored herein ($\phi = 5$), the amounts of PAHs detected approached those emitted under pyrolytic conditions in N_2 (ϕ of effectively ∞), it was assumed that an asymptotic maximum was reached thereafter. This suggests that when $\phi \rightarrow \infty$, at a given gas temperature, modest variations in ϕ will cause insignificant changes in the amount of PAHs produced. The onset of the exponential relationship between ϕ and the level of PAHs detected appears to be a function of the nature of the fuel being burned. Thus, the following sigmoidal relationship was established between ϕ and the levels of specific as well as total PAH emissions at a given gas temperature:

$$[\mathrm{PAH}] = c \times \left(\frac{1}{1 + e^{(a/\phi) - b\phi}}\right) \qquad (2)$$

where a represents a constant that influences the slope of the exponential relationship; b influences the range over which small changes in ϕ represent little or no change in the amount of PAH produced; and c represents the largest amount of PAH observed. This equation states that as $\phi \rightarrow 0$ or when $\phi \rightarrow \infty$, modest variations in ϕ will have little or no effect on the amount of PAHs produced, while throughout the remainder of the range of ϕ values the level of PAHs produced will vary exponentially with ϕ.

Using the data of Tables 3 and 4 for aerosol combustion in the VF, eq 2 was plotted for coal and tire in Figures 8 and 9, respectively. The total amounts of gas-phase PAHs as well as those for pyrene, phenanthrene, cyclopenta[*cd*]-pyrene, and benzo[*a*]pyrene were plotted. At low values of ϕ, very small amounts (if any) of PAHs are observed for either fuel. At ϕ higher than stoichiometry an exponential behavior is observed and the PAH emissions increase rapidly with small increases in ϕ. While PAH emissions for values of ϕ larger than 5 were not examined, it is presumed that

an asymptotic relationship between PAH emissions and ϕ will result. Again, this was suggested because the detected amounts of PAHs at $\phi = 5$ were in the vicinity of those detected under pyrolytic conditions in N_2 (at an equivalent ϕ of ∞). The total PAH amount also correlated well with a sigmoidal plot, but the upper asymptotic limit was not included in Figures 8 and 9 to provide an expanded scale for the individual components.

Condensed-Phase PAH Emissions. The above discussion pertains to the gas-phase PAH emissions that were adsorbed on XAD-4. Condensed-phase PAHs are listed in Tables 6 and 7. These are PAHs extracted from material collected on the filters, i.e., soot, unburned carbon, and ash. Solid-phase PAHs were only detected at fuel-rich conditions for both fuels, where combustion efficiencies are expected to be less than 80%. Hence, not all the amounts detected were generated during combustion/pyrolysis, but some may have been extracts of indigenous PAHs in the unburned fuel. It should be noted that more solid-phase PAHs were detected under severely fuel-rich conditions than under purely pyrolytic conditions in N_2.

Acknowledgments

This research was supported by EPA Grant R-819245-01-0. The authors would like to acknowledge the help provided by the Army Research Lab in Natick, MA, for the use of GC/MS. We would also like to thank Ms. Bonnie Courtmanche and Dr. Judi Steciak for their assistance with inorganic emission experiments.

Literature Cited

(1) Marks, J. *Power Eng.* **1991**, *Aug.*
(2) Serio, M. A.; Wójtowicz, M. A.; Teng, H.; Pines, D. S.; Solomon, P. R. *Preprints of Papers Presented at the 206th ACS National Meeting*, Chicago, IL, Aug 22−26, 1993; American Chemical Society: Washington, DC, 1993; Vol. 38, No. 3.
(3) Kearney, A. T. Final Report. Prepared for the Scrap Tire Management Council, Sep 1990.
(4) Atal, A.; Levendis, Y. A. *Fuel* **1995**, *74* (11), 1570.
(5) Smith, I. W. *Nineteenth Symposium (International) on Combustion*; The Combustion Institute: Pittsburgh, PA, 1982; pp 1045−1065.
(6) Smoot, L. D. In *Fossil Fuel Combustion—A Source Book*; Bartok, W. A., Sarofim, A. F., Eds.; John Wiley & Sons, Inc.: New York, 1989.
(7) Annamalai, K.; Ryan, W. *Prog. Energy Combust. Sci.* **1993**, *19*, 383−446.
(8) Annamalai, K.; Ryan, W.; Dhanapalan, S. *Prog. Energy Combust. Sci.* **1994**, *20*, 487−618.
(9) EPRI GS-7538. Prepared by Electric Power Research Institute, Palo Alto, CA, Sep 1991.
(10) Clark, C.; Meardon, K.; Russell, D. EPA-450/3-91-024 (NTIS PB92-145358). U.S. EPA: Washington, DC, Dec 1991.
(11) Pirnie, M. Prepared for the Ohio Air Quality Development Authority, May 1991.
(12) Lemieux, P. M. EPA-600-R-94-070. U.S. EPA: Washington, DC, Apr 94.
(13) Beér, J. M. *Twenty-Second Symposium (International) on Combustion*; The Combustion Institute: Pittsburgh, PA, 1988; pp 1−16.
(14) Bowman, C. T. *Twenty-Fourth Symposium (International) on Combustion*; The Combustion Institute: Pittsburgh, PA, 1992; pp 859−878.
(15) Bartok, W. A., Sarofim, A. F.; *Fossil Fuel Combustion—A Source Book*; John Wiley & Sons, Inc.: New York, 1989.
(16) Flagan, R. C.; Seinfeld, J. H. *Fundamentals of Air Pollution Engineering;* Prentice Hall: Englewood Cliffs, NJ, 1988.
(17) Pershing, D. W.; Wendt, J. O. L. *Sixteenth Symposium (International) on Combustion*; The Combustion Institute: Pittsburgh, PA, 1977; pp 389−399.
(18) Horvath, M. *Proceedings: 1991 Conference on Waste Tires as a Utility Fuel*; EPRI GS-7538; Prepared by Electric Power Research Institute: Palo Alto, CA, Sep 1991.
(19) Pope, K. M. *Proceedings: 1991 Conference on Waste Tires as a Utility Fuel*; EPRI GS-7538, Prepared by Electric Power Research Institute: Palo Alto, CA, Sep 1991.
(20) Anonymous. Oxford meets performance goals firing whole tires. *Power* **1988**, *Oct*.
(21) Makansi, J. *Power* **1992**, *Apr*.
(22) Levendis, Y. A.; Atal, A.; Steciak, J. Presented at the Twentieth International Conference on Coal Utilization and Fuel Systems, Clearwater, FL, Mar 1995.
(23) Bonfanti, L.; DeMichele, G.; Riccardi, J.; Lopez-Doriga, E. *Combust. Sci. Technol.* **1994**, *101*, 505−525.
(24) Lipkea, H. W.; Johnson, H. J. *SAE Tech. Pap. Ser.* 1978, *No. 780108*.
(25) Williams, T. P.; Bartle, K. D.; Andrews, G. E. *Fuel* **1986**, *65*, 1150.
(26) Williams, T. P.; Andrews, G. E. Bartle, K. D. *SAE Tech. Pap. Ser.* **1987**, *No. 870554*.
(27) Williams, T. P.; Abass, M. K.; Andrews, G. E. *Combust. Flame* **1989**, *75*, 1−24.
(28) Barbella, R.; Bertoli, C.; Ciajolo, A.; D'Anna, A. *Combust. Flame* **1990**, *82*, 191−198.
(29) Abass91, M. K.; Andrews, G. E.; Kennion, S. J.; Williams, T. P.; Bartle, K. D. *SAE Tech. Pap. Ser.* **1991**, *No. 910487*.
(30) Longwell, J. F. *Nineteenth Symposium (International) on Combustion*; The Combustion Institute: Pittsburgh, PA, **1982**; 1339−1350.
(31) Masclet, P.; Bresson, M. A.; Mouvier, G. *Fuel* **1987**, *66*.
(32) Garcia, J. P.; Beyne-Masclet, S.; Mouvier, G.; Masclet, P. *Atmos. Environ.* **1992**, *26A* (9), 1589−1597.
(33) Miller, C. A.; Srivastava, R. K.; Ryan, J. V. *Environ. Sci. Technol.* **1994**, *26*, 1150−1158.
(34) Nsakala, N.; Rini, M.; Cohen, M. Presented at the Twenty-First International Conference on Coal Utilization and Fuel Systems, Clearwater, FL, Mar 1996.
(35) Williams, P. T.; Taylor, D. T. *Fuel* **1993**, *72* (11), 1469−1474.
(36) Drabek, J.; Willenberg, J. *TAPPI Proc.* **1987**, 147−152.
(37) Lemieux, P. M.; Ryan, J. V. *Air Waste Manage. Assoc.* **1993**, *43*, 1106−1115.
(38) Leung, D. Y. C.; Lam, G. C. K. Presented at the 3rd Asian-Pacific International Symposium on Combustion and Energy Utilization, 1995.
(39) Atal, A.; Steciak, J.; Levendis, Y. A. *Fuel*, **1995**, *74* (4), 495.
(40) Wheatley, L.; Levendis, Y. A.; Vouros, P. *Environ. Sci. Technol.* **1993**, *27*, 2885−2895.
(41) Levendis, Y. A.; Zhu, W. G.; Wise, D. L.; Simons, G. A. *AIChE J.* **1993**, *39* (5), 761.
(42) Atal, A.; Levendis, Y. A. *Combust. Flame* **1994**, *98*, 326−349.
(43) Levendis, Y. A.; Estrada, K. R.; Hottel, H. C. Rev. Sci. Instrum. **1992**, *63*, 3608.
(44) Timothy, L. D.; Sarofim, A. F.; Beèr, J. M. *Nineteenth Symposium (International) on Combustion*; The Combustion Institute: Pittsburgh, PA, 1982; p 1123.
(45) Levendis, Y. A.; Flagan, R. C. *Combust. Sci. Technol.* **1987**, *53* (2−3), 117.
(46) Cumper, J. G.; Levendis, Y. A.; Metghalchi, M. Presented at the Symposium on Heat and Mass Transfer in Fire and Combustion Systems, ASME Winter Annual Meeting, Dallas, TX, ASME publication HTD-148, Nov 25−30, 1990.
(47) Steciak, J.; Levendis, Y. A.; Wise, D. L. *AIChE J.* **1995**, *41*, 712.
(48) Levendis, Y. A.; Courtemanche, B. NO, NO_x, and SO_2 Emissions from the Combustion of Solid Fuels. Submitted for publication.
(49) Atal, A.; Steciak, J.; Levendis, Y. A. *Proceedings of the ASME Heat Transfer Division*; HTD: San Francisco, CA, Nov 12−17, 1995; Vol. 317-2.
(50) Panagiotou, T.; Levendis, Y. A.; Delichatsios, M. A. *Combust. Sci. Technol.* **1994**, *103*, 63.
(51) Howard, J. B.; Longwell, J. P.; Marr, J. A.; Pope, C. J.; Busby, W. F.; Lafleur, A. L.; Taghizadeh, K. *Combust. Flame* **1995**, *101*, 262−270.

Received for review December 5, 1995. Revised manuscript received May 3, 1996. Accepted May 3, 1996.[⊗]

ES950910U

[⊗] Abstract published in *Advance ACS Abstracts,* July 1, 1996.